Materials and techniques for pressure calibration by resistance-jump transitions up to 500 kilobars

K. J. Dunn and F. P. Bundy

General Electric Corporate Research and Development, Schenectady, New York 12301

(Received 29 September 1977; in final form, 6 December 1977)

The resistance jump of $\alpha \rightarrow \epsilon$ transitions for Fe–V alloys up to 20-wt.% V is observed by static compression. It is used along with $\alpha \rightarrow \epsilon$ transitions for Fe–Co alloys and some other transitions as the basis for pressure calibration up to 500 kilobar.

INTRODUCTION

In the early days of research in the field of high pressure the apparatus and pressure magnitudes were such that the pressures attained could be determined by direct force over area methods. As techniques and designs for higher pressures were developed, using pistons of truncated cone or truncated-pyramid geometry with pressurized gasketing on the flanks, the cell pressure could no longer be determined directly from the force applied to the piston bases because an undetermined fraction of the applied force was borne by the gasket. In such apparatus in which the electrical resistance of the specimen could be monitored pressure calibration points could be established by observing resistance jumps associated with known first-order phase transitions in the specimen material.

As the pressure capability of various kinds of static ultrahigh pressure apparatus was increased still more by development, the problem of determining the true values of the pressures at which various first-order phase transitions occur at the higher pressure levels became more difficult. In general, two or three approaches were taken. One was to observe shock compression experiments, in which very high pressures could be reached transiently, for discontinuities in volume or density associated with phase transitions.[1] The second was to study in detail the P, V, T behavior of some simple-structured substance (like NaCl or Al) and work out a theoretical model which could be extrapolated rather reliably beyond the region of actual measurements.[2] Then, in pressure cells amenable to x-ray diffraction monitoring, the pressure could be gauged by the lattice compression of the model substance. If a resistance-monitored substance with a phase transition could be observed simultaneously in the same cell, the pressure of the transition could be established by the lattice compression of the surrounding model substance. A third approach was to insert a material having some

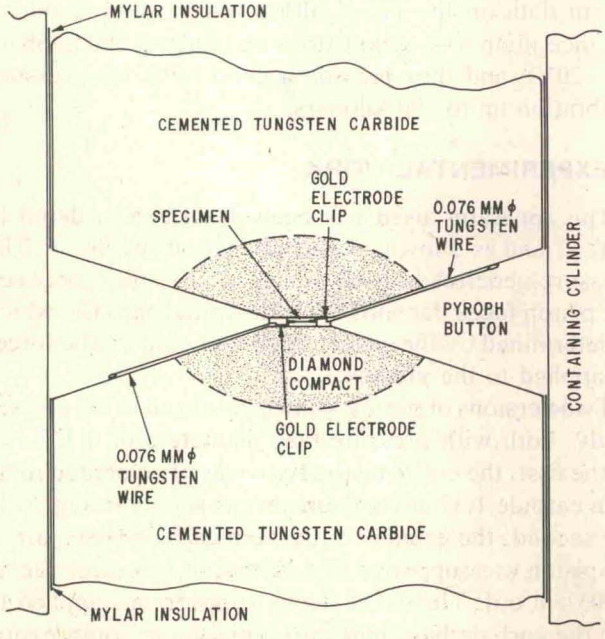

FIG. 1. Cross section of diamond-tipped opposed anvil apparatus used in the calibration experiments.

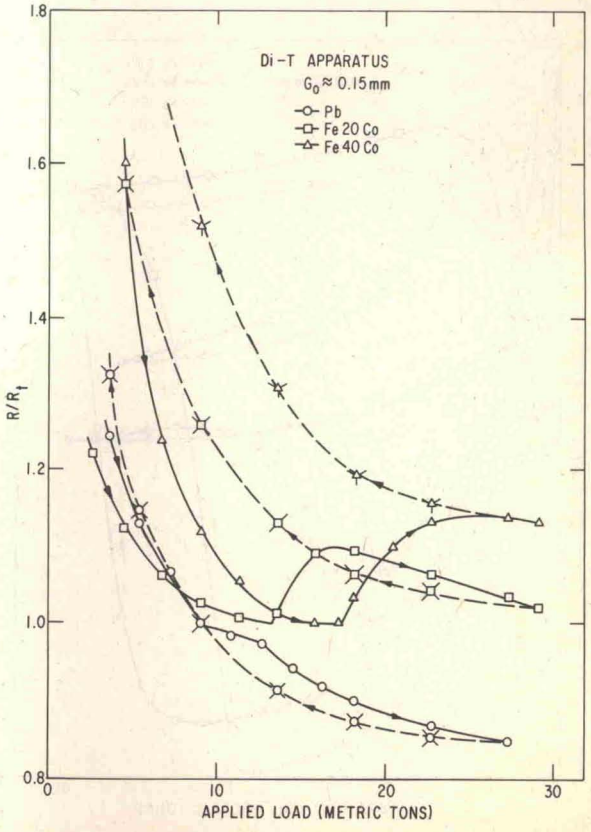

FIG. 2. Resistance versus force loading of the apparatus for specimens of Pb, Fe–20Co, and Fe–40Co in the 1.37-cm-diam apparatus.

 0034-6748/78/4903-0365$00.60

kind of optical spectrum shift with pressure along with a model compressibility material (such as ruby and NaCl) and monitor the spectral shift of the first against the lattice compression of the second.[3] Then a resistance-jump substance could be run against either the spectral-shift substance or the lattice compression substance to establish the pressure values of the resistance-jump transitions.

Historically, Bridgman suggested the first resistance-jump calibration points of Bi, Tl, Cs, Ba, etc., in his paper on resistance behavior of materials based on experiments in his opposed anvil apparatus.[4] The pressure numbers associated with these transitions were revised by Kennedy in 1960.[5] A new higher range of resistance-jump calibration points was added in 1961 by Balchan and Drickamer[6] (Fe, 131; Ba, 144; Pb, 161; Rb, 190 kilobars). As a result of the development of the NaCl compression scale by Decker[2] and others, Drickamer[7] revised the numbers for Fe, Ba, Pb, and Rb downward in 1970. In 1975 Bundy reported some newly observed resistance-jump data associated with the $\alpha \rightarrow \epsilon$ phase transitions in the Fe–Co alloys first reported by Loree *et al.*[1] as density transformations observed in shock compression experiments. These Fe–Co resistance-jump transitions were observed in a new opposed piston apparatus[8] in which the piston tips were of strongly sintered diamond powder. According to the shock compression data the Fe–40Co ($\alpha \rightarrow \epsilon$) transition occurred at about 290 kilobars. Using a sample of the same material and a Bassett-type "diamond squeezer" apparatus

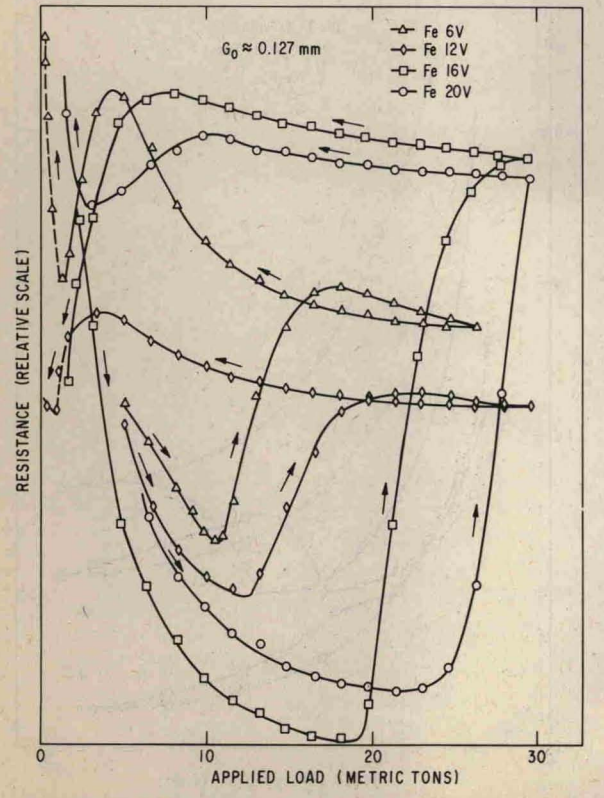

FIG. 3. Resistance versus force loading in the 1.37-cm-diam apparatus for specimens of Fe–6V, Fe–12V, Fe–16V, and Fe–20V, all at about the same G_0 in the same apparatus.

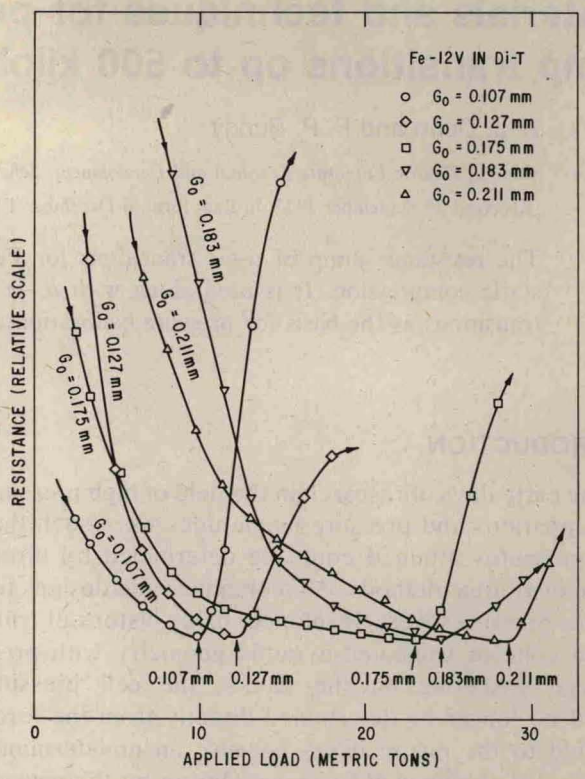

FIG. 4. Resistance versus loading for Fe–12V in the 1.37-cm-diam apparatus for a range of initial gaps, G_0.

Papantonis and Bassett[9] checked it by x-ray diffraction monitoring against NaCl. The $\alpha \rightarrow \epsilon$ transition in the Fe–40Co occurred at about 290 kilobars by the NaCl compression scale, which is about the same pressure at which NaCl starts to transform over to the CsCl structure. Thus the resistance-jumps of the $\alpha \rightarrow \epsilon$ transition in the Fe–Co alloys could be used reliably for calibration up to about 300 kilobars.

The purpose of the present paper is to present some recent data on the Fe–V alloys which show good resistance-jump $\alpha \rightarrow \epsilon$ transitions up to about 500 kilobars (Fe–20V), and thus provide a good basis for pressure calibration up to 500 kilobars.

I. EXPERIMENTAL WORK

The apparatus used has been described in detail in Ref. 8, and is shown in partial section in Fig. 1. The pressure generated at the center of the space between the piston faces depends upon the initial gap, G_0, which is determined by the gasket thickness, and by the force, L, applied to the pistons.

Two versions of the apparatus were used in the present study, both with pressure-face diameters of 0.127 cm. In the first, the entire piston base was of cemented tungsten carbide 1.37 cm in diameter, as shown in Fig. 1. In the second, the cemented tungsten carbide base part of the piston was supported by a shrunk-on tool steel sleeve, 1.905-cm o.d. This steel sleeve support was applied to put the carbide base part into initial hoop compression and thus prevent the development of hoop tension stress in the carbide during heavy axial loading. The pistons

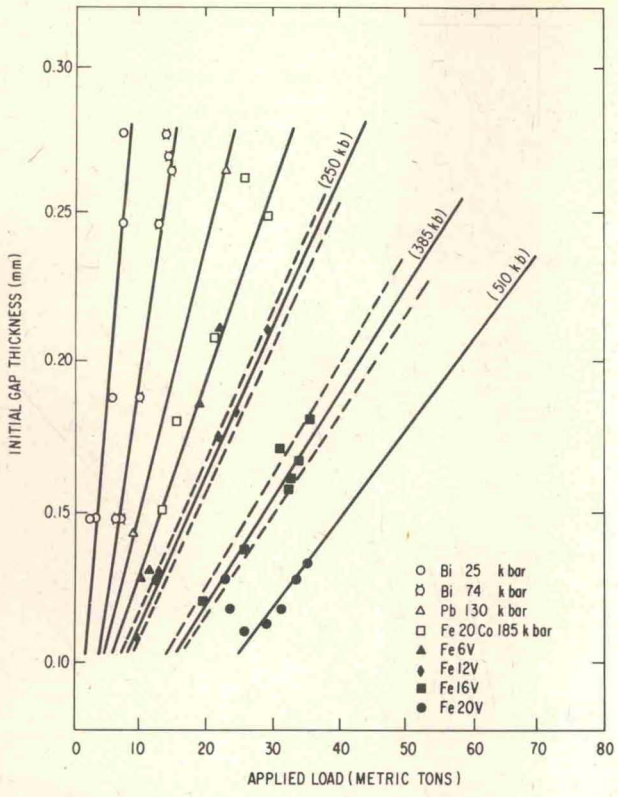

FIG. 5. Chart of G_0 vs L for the start of resistance-jump transitions of various calibration substances in the 1.37-cm-diam apparatus.

with the larger base diameter required a larger diameter cylinder and gasket, and hence, larger forces were needed to generate given face pressures.

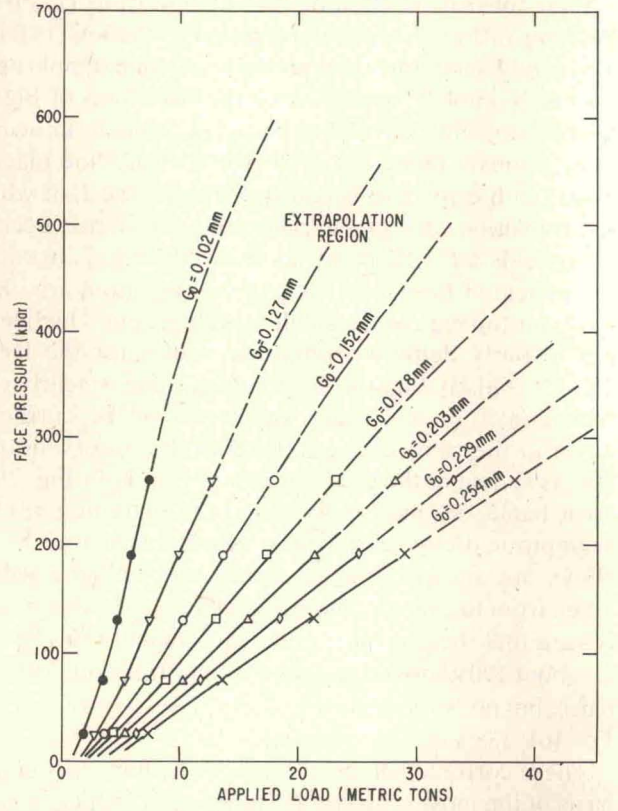

FIG. 6. P vs L, G_0 calibration chart based on well-recognized pressures below about 200–250 kilobars, and extrapolated above that.

Figure 2 shows the resistance behavior of Pb, Fe–20Co, and Fe–40Co in the 1.37-cm-diam apparatus, all at about the same initial gap conditions. For each metal there is the initial drop of resistance associated with firming up of the contacts and the cell. Then when the transition pressure is attained, the resistance increases sharply with loading until the phase transformation is complete, following which the resistance decreases slowly with increased loading. Upon unloading the reverse transition appears at much lower force loadings compared to the uploading. Because of slippage and distortion the pressure face zone does not unload at the same rate as the gasket area. This "hysteresis" behavior appears to be a common characteristic of all flank-gasketed ultrahigh pressure apparatus and is mechanical in nature. There is little reason to believe that, for a soft metal like lead, the actual pressure of the back transition is much different from that of the forward transition.

Figure 3 shows the resistance versus force loading of Fe–6V, Fe–12V, Fe–16V, and Fe–20V specimens for about the same initial gap conditions in the same apparatus. It is seen that the resistance rises associated with the $\alpha \rightarrow \epsilon$ transition are reasonably sharp, and that the usual "hysteresis" is evident in the unloading parts of the curves.

Figure 4 shows a series of experiments done in the

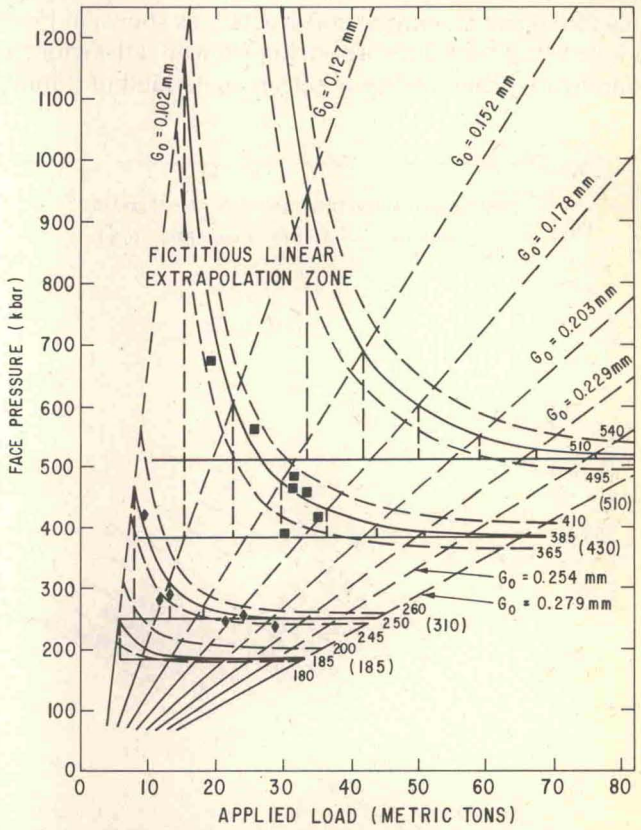

FIG. 7. Chart like Fig. 6, but ficticiously extrapolated in a linear manner. The center lines of the bands correspond to the related "Pressure lines" in Fig. 5, and the widths of the bands correspond to the widths of the data scatter bands in Fig. 5. The data points and their scatter bands are shown in Fig. 5 and Fig. 7 for the "250 kilobars" and "385 kilobars" cases. The numbers in parentheses are shock pressure values from Loree *et al.*

1.37-cm-diam apparatus with Fe–12V using different initial gaps (and hence gasket thicknesses). As mentioned above, the greater the initial gap thickness the greater the force that must be applied to the pistons to generate a given cell pressure between the faces. This is because, for the fixed taper angle of the thickness of the gasket, any change of the gap at the center changes the radial pressure distribution in the gasket. In the procedure of studying pressure calibration of the apparatus it was instructive to carry out a series of experiments for each calibration metal for a range of gaps, G_0. In this way, a family of lines could be generated on a chart showing gap versus loading force required to start the transition for each different calibrant, as shown in Fig. 5. Developing such organized sets of data is important because even with the most careful and uniform techniques of preparing and loading the cells there is some scatter of the results from the ideal functional relationship, as is evident in the chart. However, an adequate number of tests and data points establish the lines for each calibrant quite well.

II. REDUCTION OF EXPERIMENTAL DATA

If the transition pressure of each calibrant is known quite accurately in absolute terms those pressures may be assigned to the lines in Fig. 5, and from the chart a cell pressure calibration chart of P (face pressure) vs L (loading force) and G_0 may be constructed, as shown in Fig. 6. However, if the values are not known with satisfactory accuracy one can *arbitrarily* set up some kind of a formal

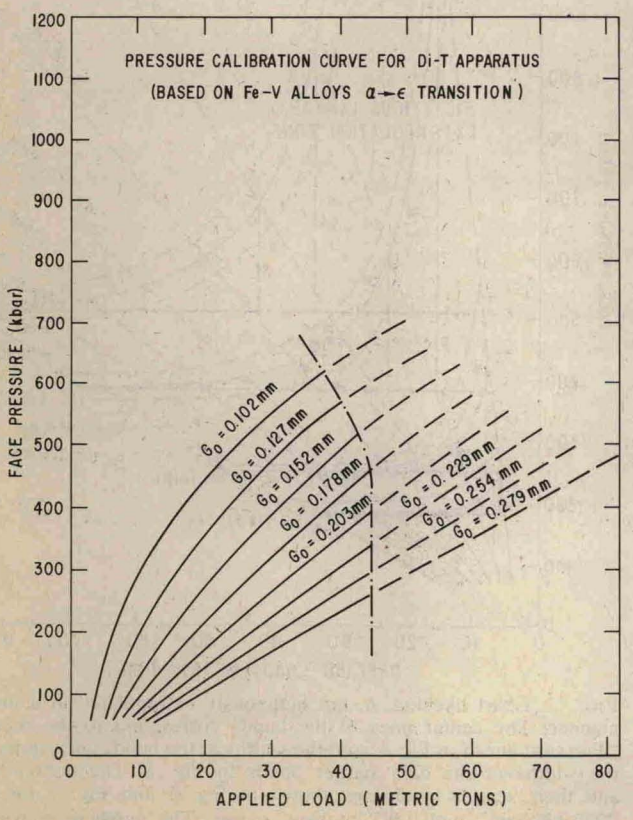

FIG. 8. Corrected, or adjusted, $P(L)$ curves for various G_0's for the 1.37-cm-diam apparatus.

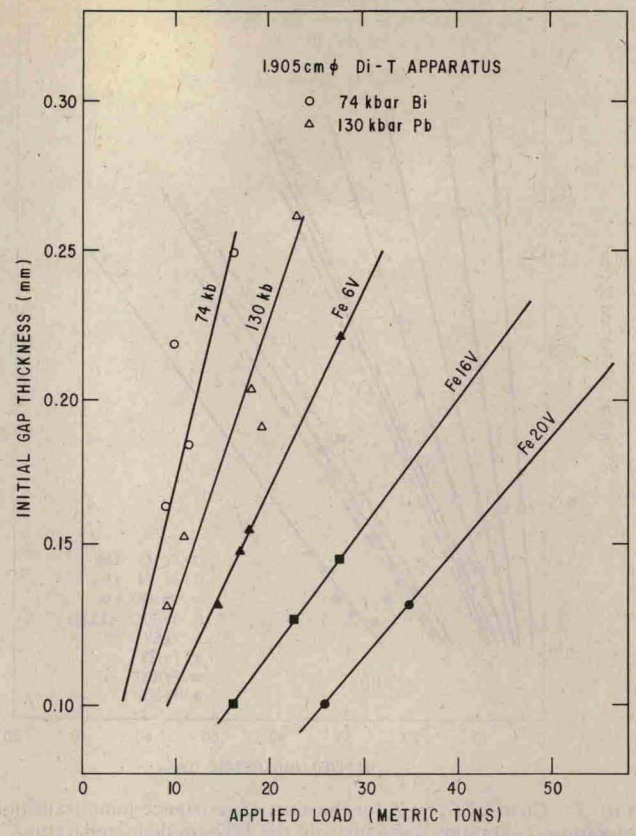

FIG. 9. Resistance-jump transition lines for various calibrants on G_0 vs L plot for the 1.905-cm-diam apparatus.

analysis procedure to develop closer probable values of the higher pressures. *One* such procedure is as follows:

First construct a chart of P vs L for various G_0's from the *lines* of Fig. 5 which correspond to the lower, fairly well established transition pressures—for example up to about 250 kilobar, as shown by the solid lines of Fig. 6. Second, extend each G_0 line linearly, (which is known to be fictitious). Third, on each extended G_0 line place a point (with error bars) corresponding to the L at which the transition of a given calibrating substance occurs. This yields a P vs L chart, as shown in Fig. 7, in which the indicated pressures for a given transition are obviously far too high at the small G_0 values, but which level out to fairly definite asymptotic values for the larger G_0's. It is likely that this asymptotic value is nearly correct, and if so, the other values should be corrected down to the same pressure level at the observed loading, as shown in the construction of Fig. 7. In Fig. 7 the error bands are indicated, and at the extreme right the asymptotic pressure transition values for the four Fe–V alloys are shown, and are compared with the values taken from the shock compression data of Loree *et al.* It is seen that there is quite good agreement of the Fe–6V (at about 190 kilobars) and the Fe–20V (at about 510 kilobars), but not so good for Fe–12V (250 vs 310 kilobars) or Fe–16V (385 vs 430 kilobars).

These corrected points for a given G_0 then become the basis of the most probable $P(L)$ curve for that G_0. Figure 8 shows the final adjusted $P(L)$ chart from the test data for the 1.37-cm-diam apparatus. The solid parts of the

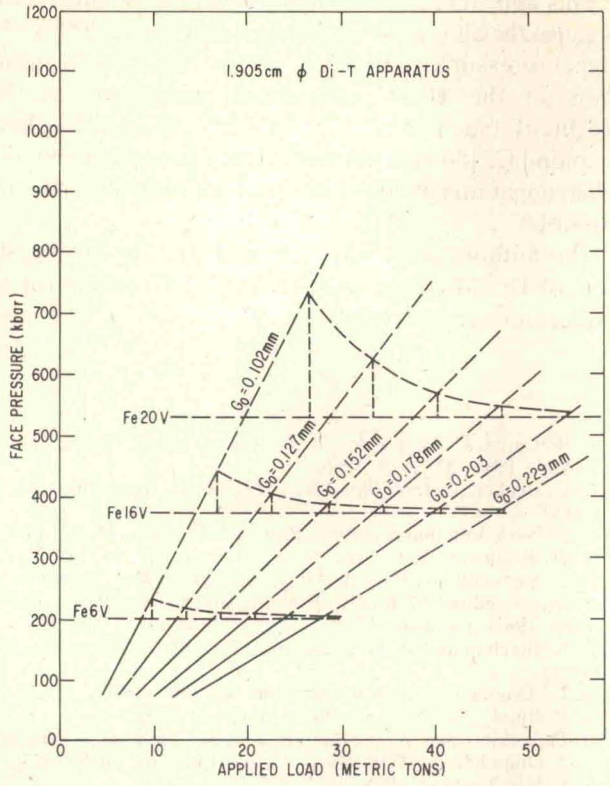

FIG. 10. P vs L construction diagram for the Fe–V alloy transitions as observed in the 1.905-cm-diam apparatus.

lines correspond to pressures actually reached in the test while the dashed parts indicate extrapolations beyond that.

A program of calibration tests of the same type was carried out for the 1.905-cm-diam apparatus with the results shown in Figs. 9–11. Although the pressure face diameters were the same in the 1.37- and the 1.903-cm-diam apparatus the loading forces to produce given face pressures are greater in the larger diameter apparatus because of its larger gasket area. Also the asymptotic values of the transition pressures for the Fe–V alloys come out slightly different in the two apparatus, but the differences are certainly well within the basic reproducibility and accuracy of the techniques involved.

III. DISCUSSION

It now appears that there are available resistance-jump pressure calibrants which cover the pressure range to slightly over 500 kilobars. These can be used to calibrate any apparatus amenable to electric resistance monitoring of the specimen. The pressure values have been cross-checked against the "NaCl scale" up to nearly 300 kilobars, and against shock compression values up to over 500 kilobars. The values of the pressure numbers assigned to the various resistance-jump transitions can be debated in terms of the correctness of the model (such as NaCl) or the shock pressure derivations and temperature corrections.

One feature of the methodology we have presented is that it can also be applied to the establishing of more reliable values for some other pressure-dependent phenomena. For example, Fig. 12 shows a G_0 vs L plot for the 1.37-cm-diam apparatus with the lines corresponding

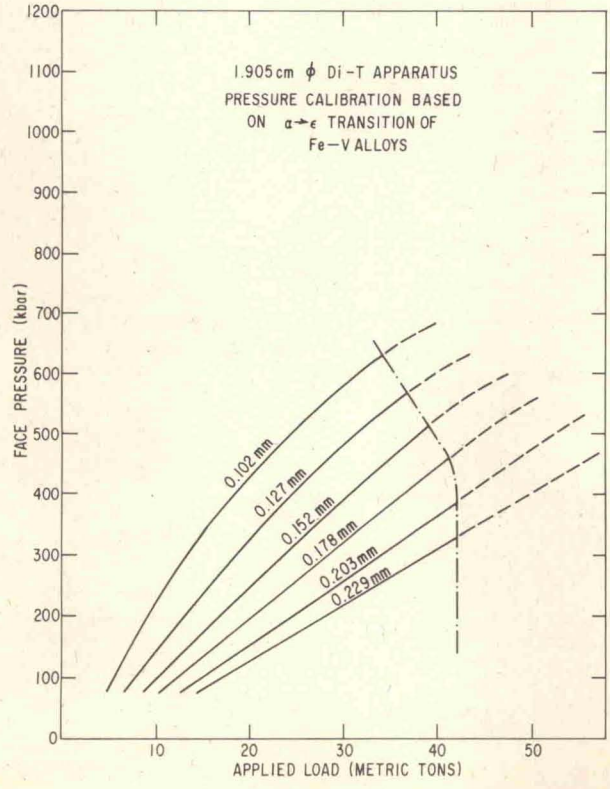

FIG. 11. Final P vs (L, G_0) calibration diagram for the 1.905-cm-diam apparatus based on all calibrants including that from Fig. 10.

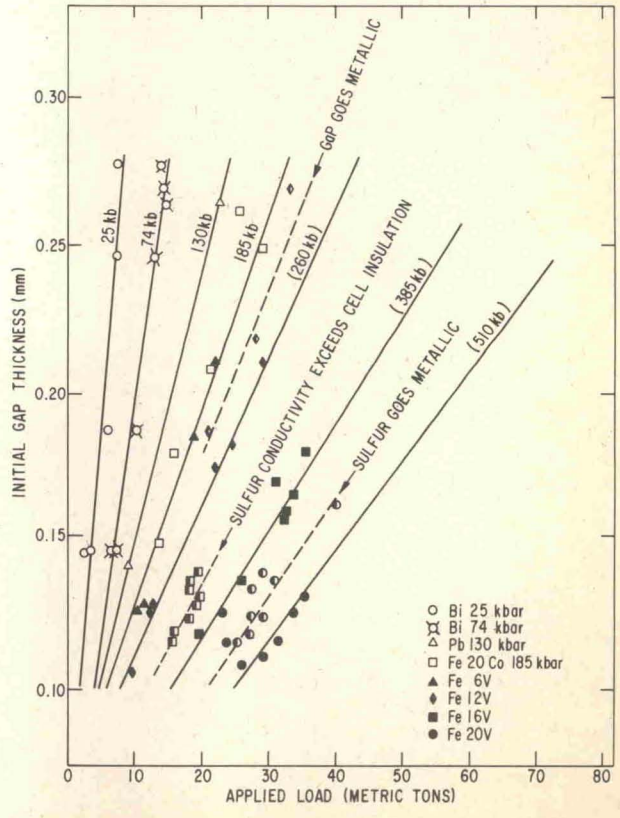

FIG. 12. G_0 vs L plot showing location of characteristic points for sulfur in comparison to the transition points for various calibrating materials.

to the various resistance-jump calibration transitions as a back-ground. Also plotted are eight points corresponding to sulfur going into the semimetallic state,[10] eight points at which the conduction of a sulfur specimen begins to exceed the leakage conduction of the cell and apparatus insulation ($\sim 10^8\ \Omega$), and three points corresponding to the transformation of GaP from diamond-cubic to the β-tin metallic form. The scatter of these points can be averaged out in a rational way on this diagram to yield pressure values of about 470, 300, and 220 kilobars, respectively.

A proposed, up-to-date, list of resistance-jump transitions which may be used for calibration of apparatus is as follows:

Bi (1-2)	25 kilobars
Ba (1-2)	53
Bi (5-6, Homan notation)	74
Fe (α-ϵ)	112
Ba (2-3)	120
Pb (1-2)	130
Fe–20Co and Fe–6V (α-ϵ)	~190
GaP (metallic transition)	~225
Fe–12V (α-ϵ)	~250
Fe–16V (α-ϵ)	~385
Fe–20V (α-ϵ)	~510

This appears to be the limit for the Fe–V alloy series, because the alloy solubility limit is just above 20% V. For higher pressure calibration points the metallic transitions in the III–V compounds suggested by Van Vechten[11] (such as BP, 420 kilobars; SiC, 660 kilobars); diamond C, 1800 kilobars; etc.) may have to be explored when apparatus of 600–1200 kilobars capability becomes possible.

The authors gratefully acknowledge the strong support of Dr. M. Aven and Dr. A. W. Urquhart for this exploratory research project.

[1] T. R. Loree, C. M. Fowler, E. G. Zukas, and F. S. Minshall, J. Appl. Phys. **37,** 1918 (1966).
[2] D. L. Decker, J. Appl. Phys. **36,** 157 (1965); J. Appl. Phys. **37,** 5012 (1966).
[3] G. J. Piermarini and S. Block, Rev. Sci. Instrum. **46,** 973 (1975).
[4] P. W. Bridgman, Proc. Am. Acad. Arts. Sci. **81,** 167 (1952).
[5] G. C. Kennedy and P. N. LaMori, *Progress in Very High Pressure Research*, edited by Bundy, Hibbard, and Strong (Wiley, New York, 1961), pp. 304–313.
[6] A. S. Balchan and H. G. Drickamer, Rev. Sci. Instrum. **32,** 308 (1961).
[7] H. G. Drickamer, Rev. Sci. Instrum. **41,** 1667 (1970).
[8] F. P. Bundy, Rev. Sci. Instrum. **46,** 1318 (1975).
[9] D. Papantonis and W. A. Bassett, J. Appl. Phys. **48,** 3374 (1977).
[10] K. J. Dunn and F. P. Bundy, J. Chem. Phys. **67,** 5048 (1977).
[11] J. A. Van Vechten, Phys. Rev. B **7,** 1479 (1973).